Semnan University

Journal of Modeling & Simulation in Electrical & Electronics Engineering (MSEEE)

Journal homepage: **https://mseee.semnan.ac.ir/**

ISSN: 2821-0786

Compact Wide-Band and Narrow-Band Microstrip Bandpass Filters Using the LC Equivalent Model

Morteza Khajavi [1] , Ebrahim Farshidi[2]*, Mohammad Soroosh[3] , and Shahrzad Ajabi[4]

***Abstract*-- This paper presents an improved design methodology for developing two types of microstrip bandpass filters, a narrowband filter and a wideband filter, employing stepped-impedance resonators (SIRs) and parallel stubs. The fundamental resonator integrates two parallel stubs and a centrally located air gap within a stepped-impedance structure. The corresponding even- and odd-mode capacitances are evaluated, and an additional SIR is coupled to the primary resonator to achieve the desired bandpass response through dimensional optimization. To verify the electromagnetic simulation results, an equivalent LC circuit model is extracted and analyzed, demonstrating strong agreement with the full-wave response. Owing to its compact geometry and structurally efficient configuration, the proposed filter is well suited for integrated microwave systems. The wideband implementation is designed to operate at a center frequency of 10.02 GHz, exhibiting an insertion loss of 1.03 dB, a return loss of 30.1 dB, and 1.33 GHz bandwidth. In contrast, the narrowband design achieves a center frequency of 2.4 GHz with an insertion loss of 0.15 dB, a return loss of 26.26 dB, and 102 MHz bandwidth.**

***Index Terms*- Microstrip Bandpass Filter, Narrowband Filter, Stepped-Impedance Resonators (Sirs), Wideband Filter.**

I. INTRODUCTION

Microwave filters are the type that provide frequency selection in communications satellite, mobile communications, radar, and electronic warfare systems in microwave frequencies. In general, the electrical efficiency of a filter is described based on return losses, insertion losses, and frequency selection in the passageway. Filters should have low insertion losses, large return losses to match the impedance well with the components connected to it [1]-[2]. In the design of microstrip filters, energy storing elements such as inductors and capacitors were conventionally used. However, with the advancement of wireless communication systems, the need for transmitting large volumes of data at high frequencies, along with the necessity of size reduction, compactness, and performance enhancement through loss improvement, has led to significant attention being paid to microstrip technology in the design of microwave filters. The design of microstrip filters is fundamentally based on three main layers: the bottom layer is metal, which serves as the ground plane; the middle layer is the dielectric substrate; and the top layer consists of specific patterns, which are referred to as resonators. Various design approaches are employed in microstrip filter design. One of the designs that has garnered considerable attention in recent research is the stepped impedance resonator (SIR). Stepped impedance resonators are essentially resonators with different impedance sections that are ultimately coupled together. The design methodology of each resonator and the manner in which they are connected to one another are critical aspects of the design process. The utilization of stepped impedance resonators contributes to size reduction, loss improvement, and enhanced overall performance of the final filter structure [3]-[4]. One of the critical challenges in the design of dual-band and multi-band filters is preventing interference between the passbands. In other words, achieving appropriate frequency selectivity through adequate isolation between bands is considered a key design technique. Isolation between passbands is realized by creating high insertion loss at frequencies located between the passbands. Logically, while insertion loss is minimized

Received; 2026-02-05 Revised; 2026-02-26 Accepted; 2026-04-21

1,2,3,4. Department of Electrical Engineering, Faculty of Engineering, Shahid Chamran University of Ahvaz, Ahvaz, Iran
*Corresponding author: farshidi@scu.ac.ir

Cite this article as:
Khajavi, M., Farshidi, E., Soroosh, M. & Ajabi, S. (2026). Compact Wide-Band and Narrow-Band Microstrip Bandpass Filters Using the LC Equivalent Model. *Journal of Modeling & Simulation in Electrical & Electronics Engineering (MSEEE)*. Semnan University Press. 6 (3), 1-8.

DOI: https://doi.org/10.22075/MSEEE.2026.40492.1251

within the passbands, it reaches a maximum value at the isolation frequency, thereby preventing signal transmission. This technique effectively mitigates interference between the information transmitted in the respective passbands [5, 6].

In [7], a new design has been proposed for the bandwidth of the bandpass filter. The compact structure of the filter is also obtained by placing a microstrip ring between two parallel. In [8], a two-band bandpass filter is presented using a winding stepped impedance resonators . What is being discussed here is the average behavior of harmonic frequencies. This dual-band filter is designed to operate at 5.25, 4.2 GHz. In [9] , a two-frequency filter is designed and manufactured with parallel connection of two bandpass filters. The authors in [10] made a double-band filter by combining a bandpass filter and a wide-band bandpass filter. But these two structures have different filter compositions in the design of two-frequency filter with relatively large dimensions. The study in [11], has used a vertical stacked structure in the design of WLAN dual-frequency filters. In [12], the designed dual-band filter uses a coupled stepped-impedance resonator pair. By placing stepped impedance resonators inside a coaxial cavity, a two-band pass filter has been reported [13] with central frequencies of 0.9 and 1.8 GHz . In [14], the stub loading theory is introduced based on the voltage distribution of the resonant mode and independent dual resonance is obtained. It is possible to design a dual-band band pass filter with compact dimensions by selecting the appropriate differential-mode [15]. In [16], a dual-band band pass filter with central frequencies of 2.33 & 4.36 GHz is presented using parallel coupled SIR resonators. In [17], SIW is used to design a dual band pass filter. In the final design of the microstrip double-band pass filter, the parallel coupled lines and simple coupled microstrip rings have been used [18]. In this paper, by presenting a design algorithm, the microstrip single-band bandpass filter is designed by selecting a suitable base resonator and of course a very simple design.

The flowchart illustrating the detailed step-by-step design procedure of the filters is presented in Fig. 1. This flowchart can be used for designing any other high-performance filters as well. This flowchart encompasses all stages of filter design, beginning with the initial steps and extending through the fabrication of the final prototype, while accounting for all essential details .Therefore, it can serve as a comprehensive guide for designers working in this field.

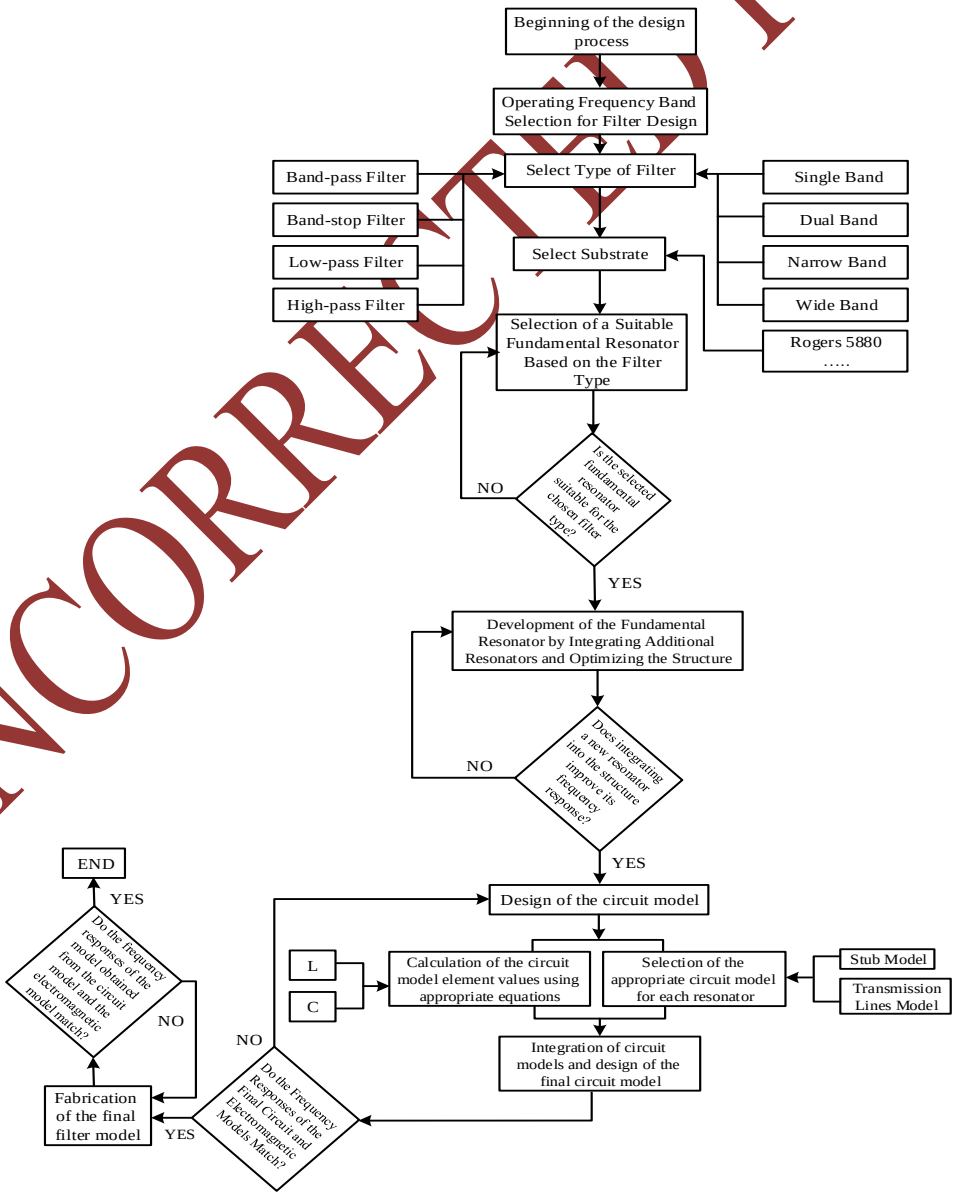

Fig. 1. Step-by-Step Flowchart for the Filter Design.

II. Basic Resonator Design

In the design of this filter, a basic stepped-impedance resonator is employed, with two parallel stubs placed at the center of its structure. Fig. 2 illustrates the stepped-impedance resonator positioned centrally within a two-stub configuration. This arrangement allows for more precise control of the filter's frequency characteristics while maintaining a compact overall structure.

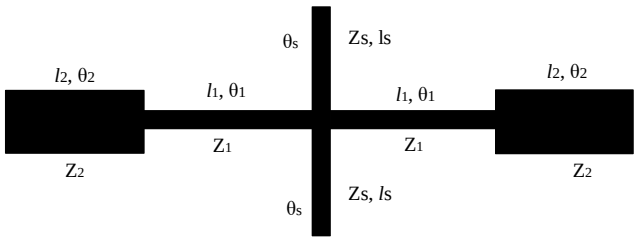

Fig. 2. A stepped impedance resonator with a stub placed in the middle of the structure [19].

The two parallel stubs with characteristic impedance ZS2 can be replaced by a single stub with impedance ZS, yielding the configuration in Fig. 3(b). Even- mode and odd-mode analysis allow determination of the corresponding capacitances and the spacing between the stubs.

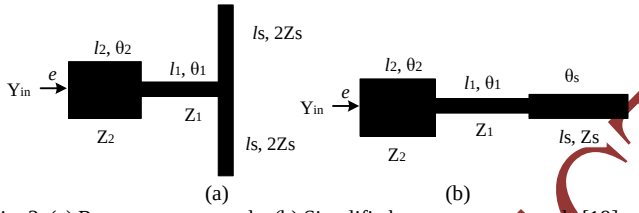

Fig. 3. (a) Resonator even mode. (b) Simplified even resonator mode [19].

The structure shown in Fig. 2 is employed to design the base resonator. Next, following the multi-stage resonator configuration in Fig. 4, an additional stepped-impedance resonator is inserted at the center of the base structure. By optimizing the dimensions of the base design, an acceptable frequency response is achieved.

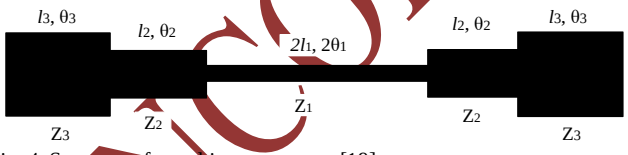

Fig. 4. Structure of a multistep resonator [19].

A base resonator is employed to design the filter. Fig. 5(a) shows a schematic of the base resonator, which consists of a simple structure with stubs separated by a gap. The frequency response of this resonator, shown in Fig. 5(b), has a center frequency of 14.32 GHz. All simulations were performed using ADS software with the Momentum solver. The substrate used is Rogers 5880 with a thickness of 15 mm, a tangent loss of 0.0009, and a dielectric constant of 2.2. The use of this substrate enables a compact design, reducing the size of the resonators and, consequently, the overall dimensions of the proposed filter.

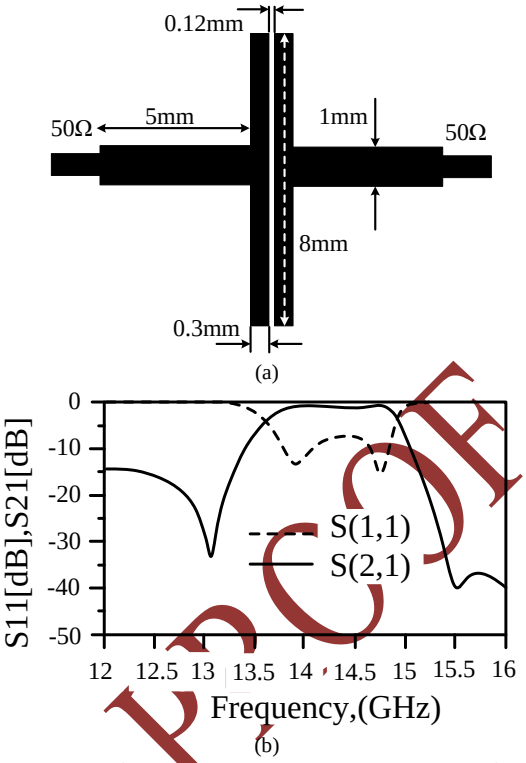

Fig. 5. (a) Schematic of the basic resonator. (b) The base resonator frequency response.

III. Narrow-Band Microstrip Filter

Given that the proposed basic resonator exhibits a bandpass-like response, one of the design objectives is to realize a bandpass filter. However, the initial structure does not provide a central frequency compatible with WLAN. To achieve a suitable operating frequency, a coupled stepped-impedance resonator is added to the base resonator. Fig. 6 illustrates the stepped-impedance resonators added to the base structure and the corresponding equivalent LC circuit.

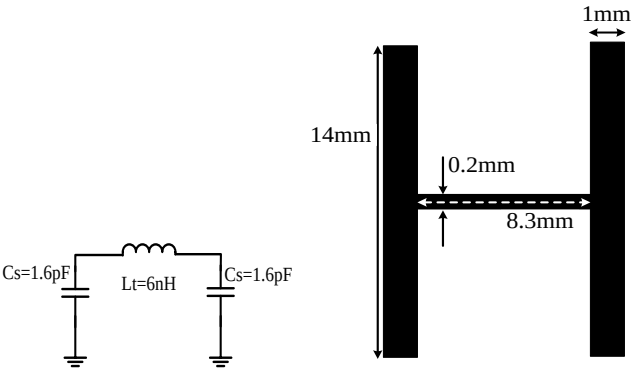

Fig. 6. Stepped impedance resonators added to the base resonator

By adding stepped-impedance resonators to the base structure, a filter with the desired frequency response is obtained, as shown in Fig. 7. The two resonators, previously illustrated in Fig. 6, are positioned between the air gap of the base resonator and the side stubs, with adjusted dimensions and displacement. The resulting filter is a single-band design, presented in Fig. 7.

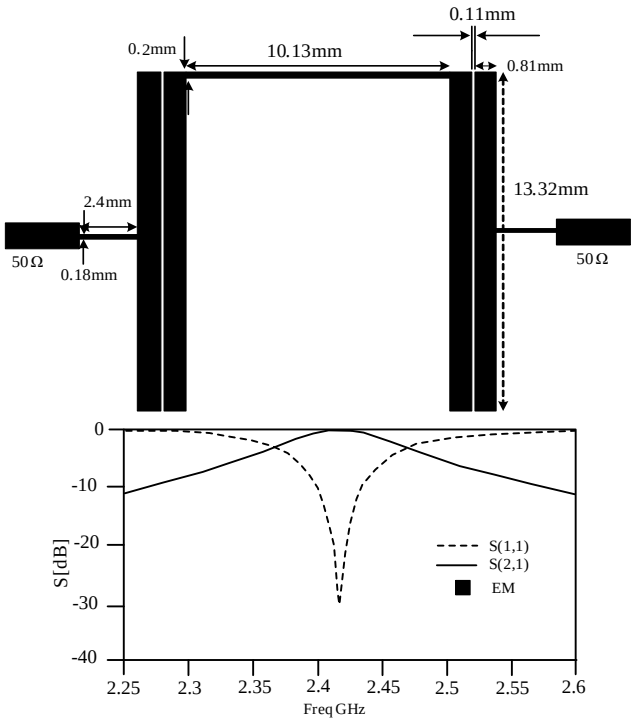

Fig. 7. The final filter is designed and its frequency response.

Finally, a filter with a center frequency of 2.4 GHz, an insertion loss of 0.15 dB, a return loss of 26.69 dB, and a bandwidth of 102 MHz was obtained.

IV. LC Model of the Narrow-Band Filter

One of the most critical steps in the design of microstrip bandpass filters is the development of an accurate equivalent circuit model that corresponds to the electromagnetic structure of each constituent resonator. While circuit models available in the literature are typically proposed for canonical resonators and simple configurations, practical filter implementations often involve the integration of multiple resonators to form the final structure. In such cases, a systematic, piecewise modeling approach is required. Specifically, the overall filter structure should be partitioned into distinct blocks, each associated with an appropriate circuit model that accurately represents its electromagnetic topology and behavior. A key challenge at this stage lies in correctly identifying the types of resonators embedded within each block and selecting the corresponding circuit topology that captures their combined response. Subsequently, the values of the circuit elements for each block must be determined. These calculations are based on four primary physical parameters: length (L), width (W), substrate thickness (h), and relative permittivity (ε_r). Using analytical formulations, these geometrical and material parameters are translated into equivalent inductance and capacitance values within the circuit model.

Upon assigning circuit models to each block and computing the element values, the individual models are integrated to form the complete equivalent circuit of the filter. The frequency response of this lumped-element model is then compared against full-wave electromagnetic simulation results. In this validation process, the most critical criterion is the accurate alignment of the passband center frequency between the circuit model and the electromagnetic structure. It is acknowledged that discrepancies may exist in other characteristics, such as insertion loss and bandwidth, due to the inherent simplifications of lumped-element models. To mitigate these discrepancies while preserving the accuracy of the center frequency alignment, the initially calculated element values are fine-tuned through a parametric optimization (sweeping) process. The ultimate objective is to achieve a satisfactory agreement between the frequency responses of the circuit model and the electromagnetic simulation, subject to the constraints imposed by the primary goal of center frequency alignment.

To design the LC circuit, the values of the inductors and capacitors are first calculated according to the relations given in [19].

$$\begin{cases} \varepsilon_{reff} = \dfrac{\varepsilon_r+1}{2} + \dfrac{\varepsilon_r-1}{2}\left\{\left(1+12\dfrac{h}{w}\right)^{-0.5} + 0.04\left(1-\dfrac{h}{w}\right)^{2}\right\} \\ Z_c = \dfrac{\eta}{2\pi\sqrt{\varepsilon_{reff}}}\ln\left(8\dfrac{h}{w}+0.25\dfrac{w}{h}\right) \end{cases} \text{for } \frac{W}{h} \leq 1 \quad (1a)$$

$$\begin{cases} \varepsilon_{reff} = \dfrac{\varepsilon_r+1}{2} + \dfrac{\varepsilon_r-1}{2}\left\{\left(1+12\dfrac{h}{w}\right)^{-0.5}\right\} \\ Z_c = \dfrac{\eta}{2\pi\sqrt{\varepsilon_{reff}}}\ln\left(8\dfrac{h}{w}+0.25\dfrac{w}{h}\right) \end{cases} \text{for } \frac{w}{h} \geq 1 \quad (1b)$$

Where $\eta=120\pi\Omega$ is the wave impedance in free space and ε_r is the relative permittivity of the substrate before the effect of the resonator layers. Now, the relationships can be summarized in the following form [19]:

$$Z_c = \frac{120\pi}{\frac{C_a}{\varepsilon_0}\sqrt{\varepsilon_{reff}}} \quad , \quad V_P = \frac{C}{\sqrt{\varepsilon_{reff}}} \quad (2a)$$

$$L_{stub} = \frac{Z_C l}{V_P} \quad , \quad C = \frac{l}{Z_C V_P} \quad (2b)$$

Here, W denotes the width of the microstrip lines, H is the substrate thickness, C is the speed of light in free space, and ε_{reff} is the effective dielectric constant. Fig. 8(a) shows the LC equivalent circuit, including the values of the inductors and capacitors, while Fig. 8(b) presents the frequency response of the final LC narrow-band filter model.

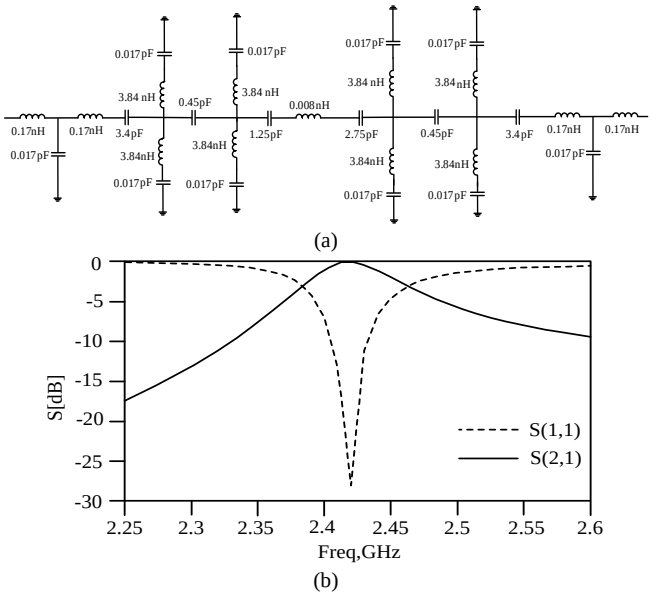

(a)

(b)

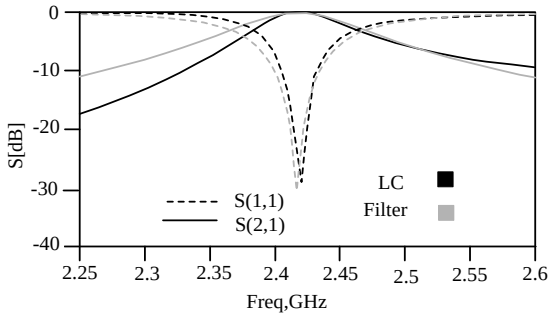

(c)

Fig. 8. (a) Equivalent circuit of LC (b) Frequency response of LC Model of the narrow-band filters. (C) Comparison of frequency response of LC model and final filter.

V. Wide-Band Microstrip Filter

By applying fundamental modifications to the basic resonator structure, including the introduction of an air gap and stubs in the central part of the structure, optimization of the transmission line dimensions and the side stubs, as well as relocating the input and output impedance matching ports to the side stubs, the narrowband single-band filter is ultimately upgraded to a wideband filter suitable for X-band applications.

Specifically, this upgrade is realized by adding stepped impedance resonators to the base resonator, producing a filter with the desired frequency response (Fig. 9(a)). The two stepped-impedance resonators shown in Fig. 6 are placed within the base resonator's air gap, with their dimensions and the position of one side stub adjusted accordingly. For a more detailed circuit-theory analysis, the LC equivalent circuit has been designed and presented, and its results are compared with the simulations.

Fig. 9(b) presents the final designed LC circuit model. Fig. 9(c) shows the fabricated prototype and its connection to the SMA ports for testing and measurement. In Fig. 9(d), the results of the electromagnetic (EM) model, the designed LC circuit model, and the final fabricated prototype are presented and compared in terms of frequency characteristics. During the fabrication process of the three-bandpass filter, a Rogers 5880 substrate with a thickness of 15 mm, low loss tangent of 0.0009, and dielectric constant of 2.2 was used.

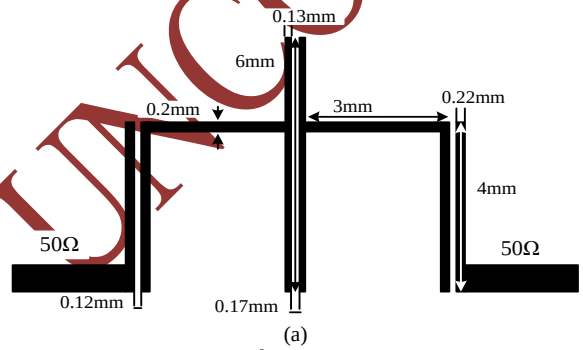

(a)

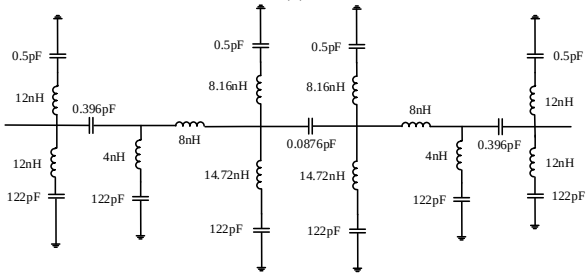

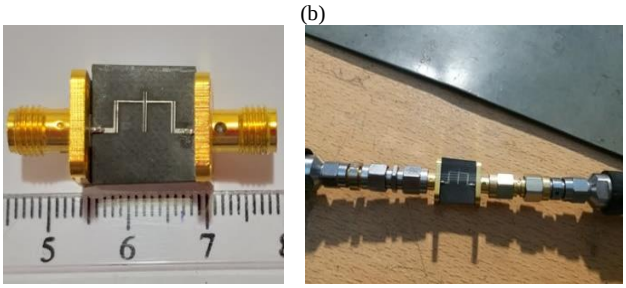

(b)

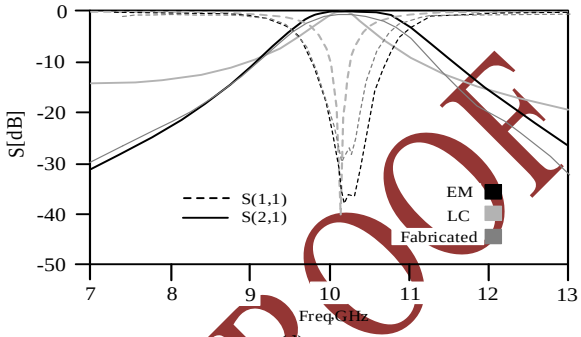

(c)

(d)

Fig. 9. (a) The final wide-band filter design along with its frequency response, (b) Equivalent circuit of LC, (c) The fabricated filter prototype, (d) Comparison of frequency response of EM model, LC Model and fabricated model of the wide-band filters.

During the measurement process, the Network Analyzer was configured with 800 points across the frequency span for both structures. Specifically, for the wideband filter, the frequency range was set from 7 GHz to 13 GHz, and for the narrowband filter, it was set from 2.25 GHz to 2.6 GHz.

TABLE I

Provides the Detailed Results of the Fabricated Prototype, the EM-Simulated Model, and the Designed LC Circuit Model, Which are Compared with Each Other.

Model	CF (GHz)	BW (GHz)	RL (dB)	IL (dB)
EM Model	10.02	1.5	38.2	0.1
Circuit Model	10.02	0.85	40.5	0.001
Fabrication	10.02	1.33	30.1	1.03

The fabrication results are strongly correlated with the type of selected substrate used in the implementation, the type of input and output impedance matching ports, the quality of the connection between these ports and the structure, as well as the precision with which the resonator patterns are realized on the substrate. Accordingly, the higher the accuracy with which the aforementioned factors are executed, the closer the frequency characteristics of the fabricated prototype will align with those of the simulated model.

To further evaluate the high selectivity of the wideband BPF, the shape factor ($S.F_{20dB/3dB}$) was employed. By slightly reformulating the normalized bandwidth as defined in [20], it is expressed as follows:

$$S.F_{20dB/3dB} = \frac{BW_{20dB\ of\ NormalizedS21}}{BW_{3dB\ of\ NormalizedS21}} \quad (3)$$

where BW_{3dB} is the bandwidth over which the filter's S21 response decreases by 3dB (usually the main operational bandwidth of the filter). BW_{20dB} is the bandwidth over which

the filter's S21 response decreases by 20dB (a measure of the filter's passband roll-off and attenuation rate). In Table II, using (3), the shape factor ($S.F_{20dB/3dB}$) of the electromagnetic (EM) model, the designed LC circuit model, and the final fabricated prototype are presented and compared. The shape factor ($S.F_{20dB/3dB}$) of the final fabricated filter is 2.3, which is considered a satisfactory result for the fabricated prototype.

TABLE II

Comparison of the quality factor between the fabricated prototype, the electromagnetic (EM) simulation model and the circuit (LC) simulation model

Parameter	Simulation EM Model	Simulation LC Model	Fabrication model
$S.F_{20dB/3dB}$	2.1	5.4	2.3

One of the key metrics in the design of microstrip filters is the quality factor (Q-factor). The quality factor directly affects frequency selectivity, insertion loss, and the overall size of the filter. By selecting appropriate materials, optimizing the resonator structure, and controlling the coupling mechanisms, a high-quality factor can be achieved, which is essential for advanced communication applications and microwave systems. For microstrip filters, the loaded quality factor, Q_L (Loaded Q-factor) is calculated using the center frequency and the bandwidth. The fundamental relationship is given as follows [19]:

$$Q_L = \frac{C_F}{BW} \quad (4)$$

In (4), Q_L denotes the loaded quality factor, C_F represents the center frequency, and BW corresponds to the passband bandwidth. In Table III, using (4), the loaded quality factor Q_L of the electromagnetic (EM) model, the designed LC circuit model, and the final fabricated prototype are presented and compared. The loaded quality factor Q_L of the final fabricated filter is 7.53, which is considered a satisfactory result for the fabricated prototype.

TABLE III

. Comparison of the QL (Loaded Q-factor) Between the Fabricated Prototype, the Electromagnetic (EM) Simulation Model and the Circuit (LC) Simulation Model

Parameter	Simulation EM Model	Simulation LC Model	Fabrication model
Q_L	6.68	11.78	7.53

In general, the quality factor relates the filter characteristics such as center frequency and bandwidth to its operational frequency band. Depending on whether the intended filter is designed for wideband or narrowband applications, the ratio of the center frequency to the bandwidth indicates the effectiveness of the design with respect to the target application. Furthermore, the shape factor represents the steepness of the frequency response; a lower shape factor corresponds to a sharper roll off, implying superior frequency selectivity and enhanced performance of the designed filter.

TABLE IV

Comparison of the Results of the Proposed Filter with a Number of References

REF	CF	SF	FBW (%)	RL (dB)	IL (dB)	SIZE (mm×mm)
1	10.04	1.48	29.11	13	2.77	40.2×28.9
2	4.3	1.46	60	18	4.1	40×34
21	5.9	1.45	16.57	10	4.7	9.1×13
22	6.47	2.01	23.27	15	2.9	20×18
23	3.09	1.28	60	17.2	0.8	39.4×27
24	2.5	1.53	50	16	0.5	96.1×35.9
25	10.28	1.92	8.1	15.9	4.31	8.3×6.8
26	8.19	2.14	34.1	25	1.2	42×28
WIDE BAND	**10.02**	**2.3**	**12.7**	**30.1**	**1.03**	**7.33×7.05**
NARROW BAND	**2.4**	**2**	**4.25**	**26.6**	**0.15**	**15.8×13.3**

RL: RETURN LOSS, IL: INSERTION LOSS, FBW: FRACTIONAL BANDWIDTH, CF: CENTRAL FREQUENCY, SF: SHAPE FACTOR

The main criteria for comparing the proposed design with other related works include the center frequency, insertion loss, return loss, and shape factor. Insertion loss is defined as the ratio of the transmitted power to the input power; in practice, the closer this ratio is to unity, the more desirable the performance. Therefore, insertion loss should be minimized as much as possible. Return loss, on the other hand, is defined as the ratio of the reflected power to the incident power. A lower reflected power is preferable to allow maximum power transmission; consequently, higher return loss values indicate less signal reflection and are thus more desirable. Finally, the shape factor represents the steepness of the frequency response. A smaller shape factor corresponds to a sharper roll-off, indicating higher selectivity and improved overall filter performance.

For the fabrication of the proposed filters, the Rogers 5880 substrate was utilized. This substrate employs alumina-based dielectric material with a thickness of 15 mm, a low loss tangent of 0.0009, and a dielectric constant of 2.2. Compared to similar studies, this substrate exhibits more favorable characteristics, which is reflected in the desirable results obtained.

VI. CONCLUSION

Initially, RF filters were realized using inductors and capacitors. In recent years, microstrip filters have gained widespread use due to their simple design process and lower fabrication cost. Most microstrip bandpass filters are typically designed for a fixed center frequency and operate in a single mode. In this work, stepped-impedance resonators with a central stub are employed to construct the base resonator. The primary contribution of this research lies in the novel design of the proposed resonator structures. The key innovations include the implementation of a symmetrical design methodology, the transformation of a narrowband configuration into a wideband response through the integration of stubs at the central section of the structure, and the optimization of critical physical dimensions. Furthermore, precise determination of the optimal junction points between transmission lines and stubs, along with the careful selection of air gap distances in both the central and lateral regions of the layout, have played a vital role in

achieving the desired frequency characteristics. These design considerations collectively form the core contributions of this work. Among the critical evaluation criteria for the proposed design are insertion loss, return loss, and shape factor. Insertion loss, defined as the ratio of transmitted power to input power, should ideally be minimized, as values closer to zero indicate higher efficiency. In this work, the measured insertion loss for the wideband and narrowband structures is 1.03 dB and 0.15 dB, respectively, demonstrating highly desirable performance. Return loss, which represents the ratio of reflected power to incident power, is another key metric; higher return loss values indicate lower reflected power and better impedance matching.

The proposed design achieves return loss values of 30.1 dB and 26.6 dB for the wideband and narrowband structures, respectively. Furthermore, the shape factor, which quantifies the steepness of the frequency response, is 2.3 for the wideband structure and 2 for the narrowband structure. These values confirm the sharp roll-off and high selectivity of the proposed filters. Overall, the results validate the effectiveness of the design approach and its suitability for modern wireless communication systems. It is worth noting that the dimensions of the designed filters, normalized to the guided wavelength, are $0.022\lambda_g \times 0.019\lambda_g$ and $0.087\lambda_g \times 0.083\lambda_g$ for the wideband and narrowband structures, respectively.

Throughout the design process, and to enhance performance, modifications are applied simultaneously to the electromagnetic (EM) model based on the finalized dimensions, while an equivalent circuit model reflecting these changes is also developed. The frequency responses of the equivalent circuit and EM models are compared and finally validated against the fabricated prototype, demonstrating excellent agreement. By introducing an additional stepped-impedance resonator between the base structures, a primary filter with the desired response is achieved. Moreover, by fine-tuning the dimensions of the side stubs in the proposed resonator and adjusting the position of one of them, both narrow-band and wide-band filters with tailored frequency responses are realized. A key advantage of the proposed design is its structural simplicity, combined with a wide bandwidth and favorable insertion and return loss characteristics.

Conflicts of Interest

The authors declare that they have no known competing financial interests or personal relationships that could have appeared to influence the work reported in this paper.

Data Availability

All data generated or analyzed during this study are included in this published article.

FUNDING STATEMENT

This research received no specific grant from any funding agency in the public, commercial, or not-for-profit sectors.

Authors' Contributions

• M. Kh:

Conceptualization, Data curation, Formal analysis, Investigation, Methodology, Project administration, Resources, Software, Supervision, Validation, Visualization, Writing – original draft, Writing – review & editing

• E.F:

Conceptualization, Data curation, Formal analysis, Investigation, Methodology, Project administration, Resources, Software, Supervision, Validation, Visualization, Writing – original draft, Writing – review & editing

• M.S:

Investigation, Methodology, Supervision, Writing – original draft, Writing – review & editing

• SH. A:

Supervision, Validation, Writing – original draft, Writing – review & editing

Statement on the use of Generative AI

We have not used artificial intelligence in any of the stages of writing the article, from design, idea, to implementation. We used AI only as a tool for language editing and clarity improvement.

References

[1] J-Y Choi, J-S Ma, and W-S Kim, "Tunable High-Selectivity Wideband Bandpass Filter Using Triple-Mode Stub-Loaded Resonators Based on Liquid Crystals," Digital Object Identifier 10.1109/ACCESS, IEEE Access, vol. 13, p. 186090, November 2025, doi: 10.1109/ACCESS.2025.186090.

[2] A. Bandyopadhyay, P. Sarkar, and R. Ghatak, "A bandwidth reconfigurable bandpass filter for ultrawideband and wideband applications," IEEE TRANSACTIONS ON CIRCUITS AND SYSTEMS. II: Express Briefs, vol. 69, no. 6, pp. 2747–2751, 2022, doi: 10.1109/TCSII.2022.3167028

[3] W. Luo, Z. Chen, Y. Zeng, L. Zhang, Y. Zhao, and C. Sun, "Design of Compact Dual-band Filter Based on Quarter Wavelength SIRs," 2022 International Applied Computational Electromagnetics Society Symposium (ACES-China), Xuzhou, China, 2022, pp. 1-3, doi: 10.1109/ACES-China56081.2022.10065035.

[4] D. Tan, W. Yang, Z. Xu, and W. Yang, "Parameter Prediction of SIR Dual Band Bandpass Filter Based on Convolutional Neural *Network,*" 2024 4th International Conference on Electronic Information Engineering and Computer Science (EIECS), Yanji, China, 2024, pp. 55-58, doi: 10.1109/EIECS63941.2024.10800526.

[5] Sh. Khani, M. Danaie, P. Rezaei, and A .Shahzadi, "Compact Ultra-Wide Upper Stopband Microstrip Dual-Band BPF Using Tapered and Octagonal Loop Resonators " Frequenz, vol. 74, no. 1-2, 2020, pp. 61-71. https://doi.org/10.1515/freq-2019-0060

[6] B. Mohammadi, A. Valizade, J. Nourinia, P. Rezaei, "Design of a compact dual-band-notch ultra-wideband bandpass filter based on wave cancellation method", IET Microwaves, Antennas & Propagation, vol.9, pp. 1-9, 2015, https://doi.org/10.1049/iet-map.2014.0372

[7] D.-J. Jung, J.-K. Lee, and K. Chang, "Wideband bandpass filter using microstrip ring," Microwave and Optical Technology Letters, vol. 53, no. 1, pp. 154–155, Jan. 2011, doi: 10.1002/mop.25678

[8] L. Guo, Z.-Y. Yu, and L. Zhang, "A dual-band band-pass filter using stepped impedance resonator," Microwave and Optical Technology Letters, vol. 53, no. 1, pp. 123–125, Jan. 2011, doi: 10.1002/mop.25648

[9] H. Miyake, S. Kitazawa, T. Ishizaki, T. Yamada, and Y. Nagatomi, "A miniaturized monolithic dual band filter using ceramic lamination technique for dual mode portable telephone," in 1997 IEEE MTT-S Int. Microwave Symp. Dig., Denver, CO, USA, Jun. 1997, pp. 789–792, doi: 10.1109/MWSYM.1997.602908

[10] L.-C. Tsai and C.-W. Hsue, "Dual-band bandpass filters using equal-length coupled-serial-shunted line and Z-transform technique," IEEE Trans. Microwave Theory Tech., vol. 52, no. 4, pp. 1111–1117, Apr. 2004, doi: 10.1109/TMTT.2004.825680

[11] N. Khajavi, S. V. Al-Din Makki, and S. Majidifar, "Design of high-performance microstrip dual-band bandpass filter,"

Radioengineering, vol. 24, no. 1, pp. 32–37, Apr. 2015, doi: 10.13164/re.2015.0032
[12] H. Zhu and A. M. Abbosh, “Single and dual band bandpass filters using coupled stepped impedance resonators with embedded coupled lines,” IEEE Microwave and Wireless Components Letters, vol. 26, no. 9, pp. 675–677, Sept. 2016, doi: 10.1109/LMWC.2016.2597180
[13] F.-C. Chen, J.-M. Qiu, S.-W. Wong, and Q.-X. Chu, “Dual band coaxial cavity bandpass filter with helical feeding structure and mixed coupling,” IEEE Microwave and Wireless Components Letters, vol. 25, no. 1, pp. 31–33, Jan. 2015, doi: 10.1109/LMWC.2014.2369965
[14] X. Wu, F. Wan, and J. Ge, “Stub-loaded theory and its application to balanced dual band bandpass filter design,” IEEE Microwave and Wireless Components Letters, vol. 26, no. 4, pp. 231–233, Apr. 2016, doi: 10.1109/LMWC.2016.2537045
[15] P. Velez, J. Bonache, and F. Martín, “Dual band balanced bandpass filter with common mode suppression based on electrically small planar resonators,” IEEE Microwave and Wireless Components Letters, vol. 26, no. 1, pp. 16–18, Jan. 2016, doi: 10.1109/LMWC.2015.2505636
[16] D. Li, J. A. Wang, Y. Liu, Z. Chen, and L. Yang, “Selectivity enhancement technique for parallel coupled SIR-based dual-band bandpass filter,” Microwave and Optical Technology Letters, vol. 63, no. 3, pp. 787–792, 2021, doi: 10.1002/mop.32672
[17] P. N. Choubey and W. Hong, “Dual band bandpass filter designed by exploiting the second-order degenerated modes of the SIW cavity,” in Proc. 2015 Asia Pacific Microwave Conf. (APMC), Nanjing, China, 2015, pp. 1–3, doi: 10.1109/APMC.2015.7411657
[18] J. Xu, K. D. Xu, M. Zhang, and Q. Chen, “Dual band bandpass filter using two simples coupled microstrip rings,” Engineering Reports, vol. 3, no. 2, p. e12288, Sept. 2020, doi: 10.1002/eng2.12288
[19] J.-S. Hong and M. J. Lancaster, Microstrip Filters for RF/Microwave Applications. New York, NY, USA: John Wiley & Sons, 2001, ISBN: 978 0471388777
[20] K. Hashimoto, M. Ueda, O. Kawachi, H. Ohmori, O. Ikata, H. Uchishiba, T. Nishihara, and Y. Satoh, “Development of ladder-type SAW RF filter with high shape factor,” in Proc. IEEE Ultrason. Symp. Int. Symp., vol. 1, Nov. 1995, pp. 113–116
[21] J. Torrecilla, C. Marcos, V. Urruchi, J. M. Sánchez Pena, and O. Chojnowska, “Liquid crystal dual mode band pass filter with improved performance,” Opto Electronics Review, vol. 23, no. 2, pp. 121–125, Jun. 2015, doi: 10.1515/oere 2015 0020
[22] Y. Liu, D. Jiang, W. Cao, T. Yang, L. Xia, and R. Xu, “Microwave tunable split ring resonator bandpass filter using nematic liquid crystal materials,” ELSEVIER-Optik, vol. 127, no. 21, pp. 10216–10222, Nov. 2016, doi: 10.1016/j.ijleo.2016.08.034
[23] X.-K. Bi, X. Zhang, S.-W. Wong, S.-H. Guo, and T. Yuan, “Synthesis design of Chebyshev wideband band pass filters with independently reconfigurable lower passband edge,” IEEE Trans. Circuits Syst. II: Express Briefs, vol. 67, no. 12, pp. 2948–2952, Dec. 2020, doi: 10.1109/TCSII.2020.3023459
[24] M. A. Sánchez Soriano and C. Quendo, “Systematic design of wideband bandpass filters based on short circuited stubs and λ/2 transmission lines,” IEEE Microwave and Wireless Components Letters, vol. 31, no. 7, pp. 849–852, Jul. 2021, doi: 10.1109/LMWC.2021.3076924
[25] J. Y. Choi, J. S. Ma, H. Oh, and W. S. Kim, “A reconfigurable narrow band bandpass filter using electrically coupled open loop resonators based on liquid crystals,” J. Phys. D: Appl. Phys., vol. 46, no. 46, p. 465307, 2024, doi: 10.1088/1361 6463/ad6dd0
[26] H. Nimehvari Varcheh, P. Rezaei, and S. Kiani, "A modified Jerusalem microstrip filter and its complementary for low phase noise X-band oscillator," International Journal of Microwave and Wireless Technologies, Vol. 15, pp. 1707–1716, Dec. 2023, doi: 10.1017/S1759078723000703.